

## SIX2 and BMP4 Mutations Associate With Anomalous Kidney Development

Stefanie Weber,\* Jaclyn C. Taylor,<sup>†</sup> Paul Winyard,<sup>‡</sup> Kari F. Baker,<sup>†</sup> Jessica Sullivan-Brown,<sup>†</sup> Raphael Schild,\* Tanja Knüppel,\* Aleksandra M. Zurowska,<sup>§</sup> Alberto Caldas-Alfonso,<sup>¶</sup> Mięczysław Litwin,<sup>¶</sup> Sevinc Emre,<sup>\*\*</sup> Gian Marco Ghiggeri,<sup>††</sup> Aysin Bakkaloglu,<sup>‡‡</sup> Otto Mehls,\* Corinne Antignac,<sup>§§</sup> Escape Network,<sup>¶¶</sup> Franz Schaefer,\* and Rebecca D. Burdine<sup>†</sup>

\*Pediatric Nephrology, University Children's Hospital Heidelberg, Germany; <sup>†</sup>Department of Molecular Biology, Princeton University, New Jersey; <sup>‡</sup>Institute of Child Health, University College London, London, United Kingdom; <sup>§</sup>Pediatric Nephrology Department, Medical University of Gdansk, Gdansk, Poland; <sup>¶</sup>Department of Pediatrics, Faculdade de Medicina do Porto, Porto, Portugal; <sup>¶¶</sup>Nephrology and Kidney Transplantation Department, Children's Memorial Health Hospital, Warsaw, Poland; <sup>\*\*</sup>Department of Pediatrics, Istanbul Medical Faculty, University of Istanbul, Istanbul, Turkey; <sup>††</sup>Laboratory on Pathophysiology of Uremia, Istituto Giannina Gaslini, Genova, Italy; <sup>‡‡</sup>Hacettepe University Faculty of Medicine, Ankara, Turkey; <sup>§§</sup>Inserm U574, Hôpital Necker-Enfants Malades, Université René Descartes, Paris, France; and <sup>¶¶</sup>Department of Genetics, Hôpital Necker-Enfants Malades, Université René Descartes, Paris, France

### ABSTRACT

Renal hypodysplasia (RHD) is characterized by reduced kidney size and/or maldevelopment of the renal tissue following abnormal organogenesis. Mutations in renal developmental genes have been identified in a subset of affected individuals. Here, we report the first mutations in *BMP4* and *SIX2* identified in patients with RHD. We detected 3 *BMP4* mutations in 5 RHD patients, and 3 *SIX2* mutations in 5 different RHD patients. Overexpression assays in zebrafish demonstrated that these mutations affect the function of *Bmp4* and *Six2* *in vivo*. Overexpression of zebrafish *six2.1* and *bmp4* resulted in dorsalization and ventralization, respectively, suggesting opposing roles in mesendoderm formation. When mutant constructs containing the identified human mutations were overexpressed instead, these effects were attenuated. Morpholino knockdown of *bmp4* and *six2.1* affected glomerulogenesis, suggesting specific roles for these genes in the formation of the pronephros. In summary, these studies implicate conserved roles for *Six2* and *Bmp4* in the development of the renal system. Defects in these proteins could affect kidney development at multiple stages, leading to the congenital anomalies observed in patients with RHD.

*J Am Soc Nephrol* 19: 891–903, 2008. doi: 10.1681/ASN.2006111282

Renal hypodysplasia (RHD) comprises common developmental defects of the kidney accounting for more than 20% of pediatric end-stage renal disease.<sup>1</sup> RHD is characterized by a reduction in nephron number, a small overall kidney size, and/or a maldevelopment of the renal tissue leading to hypoplastic or dysplastic kidneys with/without cystic changes.<sup>2</sup> So far, little is known about its molecular pathogenesis. Numerous transgenic animal models for renal developmental genes present with phenotypes highly reminiscent of human RHD and a number of human gene mutations have

Received November 27, 2006. Accepted October 3, 2007.

Published online ahead of print. Publication date available at www.jasn.org.

S.W. and J.C.T. contributed equally to this work.

<sup>¶¶</sup>See Appendix.

**Correspondence:** Dr. Franz Schaefer, Pediatric Nephrology Division, Hospital for Pediatric and Adolescent Medicine, University of Heidelberg, Im Neuenheimer Feld 150, 69120 Heidelberg, Germany. Phone: 49-6221-563-2396; Fax: 49-6221-56-4203; e-mail: franz.schaefer@med.uni-heidelberg.de or Dr Rebecca D. Burdine, Department of Molecular Biology, Princeton University, Washington Road, Mof 433, Princeton, NJ 08544. Phone: 609-258-7515; Fax: 609-258-1343; e-mail: rburdine@princeton.edu

Copyright © 2008 by the American Society of Nephrology

been associated with hereditary RHD, including *PAX2*, *EYA1*, and *HNF-1 $\beta$* . However, mutations in these genes were only identified in a fraction of RHD patients.<sup>1</sup>

Ureteric budding (UB) into the metanephric mesenchyme (MM) constitutes a crucial step during early kidney development and is regulated by the cooperative action of a complex gene network, alterations of which lead to impaired ureterorenal development and RHD.<sup>3</sup> Recent data suggest that *Six2* participates in this regulative network.<sup>4</sup> *Six2*, homologous to the *Drosophila* homeobox gene *sine oculis*, is a member of the vertebrate *Six* gene family that play important roles in early organogenesis.<sup>5</sup> *Six1*, *Six2*, and *Six5* are all expressed in the developing kidney,<sup>6</sup> and human mutations in *SIX1* and *SIX5* have been identified in patients with *EYA1*-negative Branchio-oto-renal (BOR) syndrome that is characterized by RHD, cervical fistulae, and ear anomalies.<sup>7,8</sup> The role of *Six2* for kidney development is further supported by the phenotype of the *Six2* knockout mouse that presents with severe dysplasia of the kidneys comparable to human RHD.<sup>4</sup> Microarray studies indicated that murine *Six2* expression in the MM is highly upregulated at E12.5,<sup>9</sup> the stage of UB, together with *Gdnf* and members of the Hox families *Hoxa 11* and *Hoxd 11*, which are crucial for normal kidney development. *Gdnf* is the critical paracrine signal released by the MM to activate UB via activating the c-Ret receptor tyrosine kinase,<sup>10</sup> and *Six2* is thought to act upstream of *Gdnf*, enhancing *Gdnf* expression.<sup>11</sup>

In contrast to *Six2*, *Bmp4* is an inhibitor of *Gdnf* function.<sup>12</sup> *Bmp4* is a member of the TGF- $\beta$  superfamily and has been implicated in several aspects of embryonic development by regulating cell proliferation, differentiation, and apoptosis.<sup>13,14</sup> It is one of the key regulators of UB inhibiting ectopic ureteric bud outgrowth and promoting ureter elongation.<sup>12</sup> *Bmp4* is further continuously expressed beyond the stage of UB throughout the embryonic development of the kidney and urinary system.<sup>15</sup> The striking similarity of murine knockout phenotypes of *Six2* and *Bmp4* to human malformations of the kidney promoted the idea of a specific role of *SIX2* and *BMP4* for human RHD.

To examine the role of *Six2* and *Bmp4* for kidney nephro-

genesis we performed *six2* and *bmp4* knockdown and overexpression studies in *Danio rerio* (zebrafish) and mutational analysis of the human *SIX2* and *BMP4* genes in 250 pediatric patients with RHD. Here, we report on the first human mutations identified in *SIX2* and *BMP4* in 10 unrelated patients, and we show that these mutations reduce *Six2* and *Bmp4* function in a zebrafish overexpression assay. Finally, morpholino (MO) knockdown studies indicate that loss of *six2* and *bmp4* results in disturbed pronephric development in zebrafish, suggesting conserved roles for these genes in renal development.

## RESULTS

### Human Mutations Identified in *SIX2* and *BMP4*

We identified 3 different heterozygous *SIX2* missense mutations in 5 unrelated RHD patients (Leu43Phe, Pro241Leu, Asp276Asn; Table 1; Figure 1). None of the mutations was identified in 300 control chromosomes. All *SIX2* mutations locate to highly conserved amino acid residues and affect the six domain (SD) (Leu43Phe, patient 1) or the *SIX2*-specific C-terminal domain (CD) (Pro241Leu, patients 2 to 4; Asp276Asn, patient 5; Figure 2). Statistical analysis predicts the loss of a SH3 binding site in *Six2* by the Pro241Leu exchange.

Renal phenotypes of patients 1 to 5 are listed in Table 1. Analysis of family members displayed parental heterozygous mutation carriers with unsuspecting clinical course and normal renal ultrasound (father of P2, mother of P3), indicating a low degree of penetrance (Table 1). No *de novo* mutations were identified in the families examined for *SIX2*.

Mutational analysis of the *BMP4* gene revealed 3 different missense mutations in *BMP4* in 5 unrelated RHD patients (Ser91Cys, heterozygous in patients 6 and 7; Thr116Ser, heterozygous in patient 8; Asn150Lys, heterozygous in patient 9 and homozygous in patient 10; Table 1; Figure 1). All 3 mutations locate to the prodomain of *Bmp4* and were not identified in 300 control chromosomes (Figure 2). Results of renal ultrasound for patients 6 to 10 are listed in Table 1. *BMP4* analysis of

**Table 1.** Genotype and phenotype of RHD affected individuals

Index Patient <sup>a</sup>	Origin	<i>SIX2</i> Mutation (nucleotide) <sup>b</sup>	<i>SIX2</i> Mutation (amino acid)	Kidney Ultrasound <sup>c</sup>
P1	Poland	402 C->T (pnt)	Leu43Phe (het)	DYS(l)/VUR(r)
P2	Poland	997 C->T (F)	Pro241Leu (het)	CYS-DYS(r,l)/VUR(r,l)
P3	Germany	997 C->T (M)	Pro241Leu (het)	CYS-DYS(r,l)
P4	Italy	997 C->T (pnt)	Pro241Leu (het)	HYPO(r)/VUR(r)
P5	Portugal	1100–1101 GG->AA (pnt)	Asp276Asn (het)	CYS-DYS(r,l)/HYPO(r)
		<i>BMP4</i> mutation (nucleotide) <sup>b</sup>	<i>BMP4</i> mutation (amino acid)	
P6	Poland	272 C->G (pnt)	Ser91Cys (het)	AGEN(r)
P7	Germany	272 C->G (F)	Ser91Cys (het)	DYS(l)/VUR(r)
P8	Turkey	347 C->G (de novo)	de novo Thr116Ser (het)	HYPO(r)/VUR(l)
P9	Turkey	450 C->G (pnt)	Asn150Lys (het)	HYPO(r)
P10	Turkey	450 C->G (F,M)	Asn150Lys (homo)	CYS-DYS(r,l)

<sup>a</sup>Patients, n = 250; controls, n = 150.

<sup>b</sup>Transmitted from father (F), mother (M), de novo, or parents not tested (pnt).

<sup>c</sup>DYS, dysplasia; VUR, vesicoureteral reflux; CYS-DYS, cystic dysplasia; HYPO, hypoplasia; AGEN, agenesis; l, left; r, right.

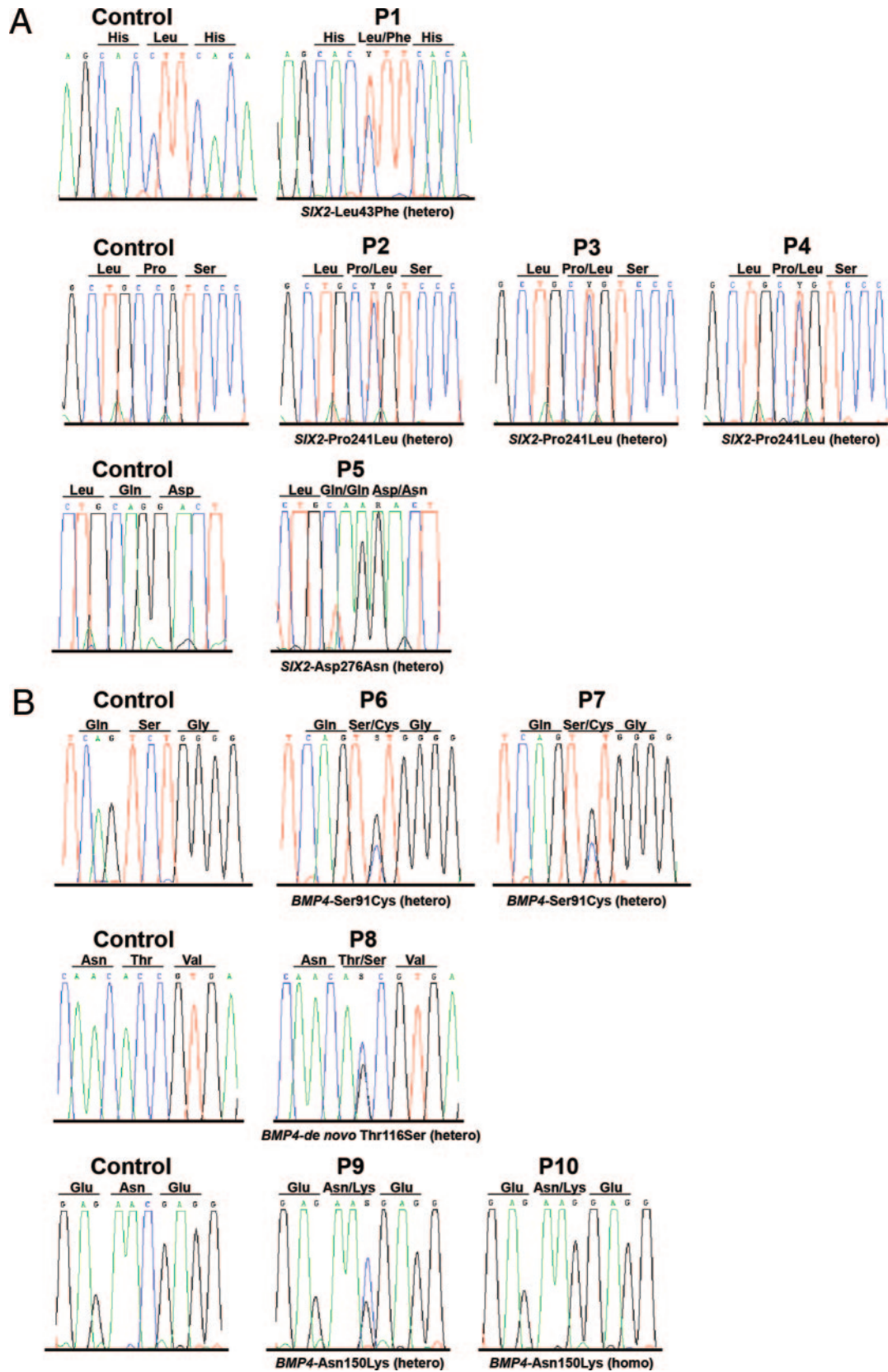


**Figure 1.** Human mutations identified in *SIX2* and *BMP4*. *SIX2* (A) and *BMP4* (B) DNA sequencing results are shown for all index patients and healthy controls.

**A Six2**

	Leu43Phe ↓				
Homo sapiens	MSMLPTFGGT	QEQVACVCEV	LQGGGNIERI	GRFLWSLPAC	EHLHKNESVL
Mus musculus	MSMLPTFGGT	QEQVACVCEV	LQGGGNIERI	GRFLWSLPAC	EHLHKNESVL
Danio rerio	MSMLPTFGGT	QEQVACVCEV	LQGGGNIERI	GRFLWSLPAC	EHLHKNESVL
	Six domain				
Homo sapiens	KAKAVVAFHR	GNFRELYKIL	ESHQFSFHHH	AKLQQLWLKA	HYIEAEKLRG
Mus musculus	KAKAVVAFHR	GNFRELYKIL	ESHQFSFHHH	AKLQQLWLKA	HYIEAEKLRG
Danio rerio	KAKAVVAFHR	GNFRELYKIL	ESHQFSFHHH	PKLQQLWLKA	HYIEAEKLRG
	-----				
Homo sapiens	RFLGAVGKYR	VRKFFFLPRS	IWDGEETS3YC	FKEKRSRSLR	EMVYHNPPYS
Mus musculus	RFLGAVGKYR	VRKFFFLPRS	IWDGEETS3YC	FKEKRSRSLR	EMVYHNPPYS
Danio rerio	RFLGAVGKYR	VRKFFFLPRS	IWDGEETS3YC	FKEKRSRSLR	EMVYHNPPYS
	-----				
	Homeobox domain				
Homo sapiens	PREKRELAER	TGLTTTQVSH	WFKNRFRQDR	AAEAKERENN	ENSHNSHSHH
Mus musculus	PREKRELAER	TGLTTTQVSH	WFKNRFRQDR	AAEAKERENN	ENSHNSHSHH
Danio rerio	PREKRELAER	TGLTTTQVSH	WFKNRFRQDR	AAEAKERENN	ENSHNSHSHH
	-----				
	Pro241Leu ↓				
Homo sapiens	---LNGSGK	SVLGSSEDEK	TFSGTFPHSS	SSPALLLS-E	FPFGLPSLHS
Mus musculus	LASSLNGSGK	SVLGSSEDEK	TFSGTFPHSS	SSPALLLSPE	FPFGLPSLHS
Danio rerio	LTSSMNGH-N	TLGSSDIDR	TFSGTGDHT	SSPALLITSN	S--GL-SLHG
	-----				
	Asp276Asn ↓				
Homo sapiens	LGHFPGPSAV	FVFPVGGGGA	DPLQHHHGLQ	DSLINPMSAN	LVDLGS
Mus musculus	LGHFPGPSAV	FVFPVGGGGA	DPLQHHHGLQ	DSLINPMSAN	LVDLGS
Danio rerio	LAFEPGSAI	FVFSV-----	DSVHHHSHH	DTLINPMSH	LVDLGS

**B Bmp4**

	Preprodomain				
Homo sapiens	MFPGRMMLV	VLLCQVLLGG	ASHASLIPEE	GKKKVAEIQG	HAGGRRSGGS
Mus musculus	MFPGRMMLV	VLLCQVLLGG	ASHASLIPEE	GKKKVAEIQG	HAGGRRSGGS
Xenopus tropicalis	MFPGRMMLV	ILLCQVLLGG	THASLIPEE	GKKK--VAE	ICGGRSAGS
Danio rerio	MFPGRMMLV	ILLCQVLLGE	SYASLIPEE	GKKK-----	-SALHLAGE
	-----				
	Ser91Cys ↓				
Homo sapiens	HELLRDFEAT	LQMFGLRRR	QFQSKSAVIP	DYMRDLRYLQ	SSEEEEE-QI
Mus musculus	HELLRDFEAT	LQMFGLRRR	QFQSKSAVIP	DYMRDLRYLQ	SSEEEEEQGS
Xenopus tropicalis	NELLRDFEAT	LQMFGLRRR	QFQSKSAVIP	AYMRDLRYLQ	SAAEED--L
Danio rerio	HELLRDFEAT	LLHMEGLRRR	RFSSHSAVIP	CYLLDLRYLQ	SSELEAG-A
	-----				
	Thr116Ser ↓				
Homo sapiens	HDTSGLEYPER	PASRANTVRS	FHHEEHLNI	PG-TSENSAF	RFLFNLSSTP
Mus musculus	HDTSGLEYPER	PASRANTVRS	FHHEEHLNI	PG-TSENSAF	RFLFNLSSTP
Xenopus tropicalis	HDTSGLEYPER	PASRANTVRS	FHHEEHLNI	PG-TSENSAF	RFLFNLSSTP
Danio rerio	HDTSGLEYPER	PASRANTVRS	FHHEEHLNI	PG-TSENSAF	RFLFNLSSTP
	-----				
	Asn150Lys ↓				
Homo sapiens	ENRIVSSAEL	RLRFQGVDDQ	PD-----WER	GFHRINIYEV	MKPPAEVWFG
Mus musculus	ENRIVSSAEL	RLRFQGVDDQ	PD-----WBO	GFHRINIYEV	MKPPAEVWFG
Xenopus tropicalis	ENRIVSSAEL	RLYRQVDDQ	PD-----WEE	GFHRINIYEV	MKE--ITASG
Danio rerio	EDDELSTAEI	RYRQVDDQ	FSDPDQTDG	GLHRINIYEV	LKAE---REG
	-----				
	Prodomain				
Homo sapiens	FTTHGGQHRV	ISR-SLFGSR	ENRQRLRPLL	VTFGHGDRG	ALTRPRRKH
Mus musculus	FTTHGGQHRV	ISR-SLFGSR	ENRQRLRPLL	VTFGHGDRG	ALTRPRRKH
Xenopus tropicalis	FTTHGGQHRV	ISR-SLFGSR	ENRQRLRPLL	VTFGHGDRG	ALTRPRRKH
Danio rerio	FTTHGGQHRV	ISR-SLFGSR	ENRQRLRPLL	VTFGHGDRG	ALTRPRRKH
	-----				
	Mature domain				
Homo sapiens	SPKHHQQRAR	KKKNKCRHRS	LYVDFSDVGV	NDWIVAPPGY	QAFYCHGDCR
Mus musculus	SPKHHQQRAR	KKKNKCRHRS	LYVDFSDVGV	NDWIVAPPGY	QAFYCHGDCR
Xenopus tropicalis	KRSFKQQRAR	KKKNKCRHRS	LYVDFSDVGV	NDWIVAPPGY	QAFYCHGDCR
Danio rerio	KRSFKQQRAR	KKKNKCRHRS	LYVDFSDVGV	NDWIVAPPGY	QAFYCHGDCR
	-----				
Homo sapiens	FPLADHLSST	NHAIVQTLVN	SVNHSIPRAC	CVPTLSAITS	MLYLDYDQV
Mus musculus	FPLADHLSST	NHAIVQTLVN	SVNHSIPRAC	CVPTLSAITS	MLYLDYDQV
Xenopus tropicalis	FPLADHLSST	NHAIVQTLVN	SVNHSIPRAC	CVPTLSAITS	MLYLDYDQV
Danio rerio	FPLADHLSST	NHAIVQTLVN	SVNHSIPRAC	CVPTLSAITS	MLYLDYDQV
	-----				
Homo sapiens	VLKHYQEMV	EGCGCR			
Mus musculus	VLKHYQEMV	EGCGCR			
Xenopus tropicalis	VLKHYQEMV	EGCGCR			
Danio rerio	VLKHYQEMV	EGCGCR			

**Figure 2.** Six2 and Bmp4 sequence alignments. (A) Alignment of Six2 amino acid (AA) sequences depicting the AA sites affected by the missense mutations identified in this study (Leu43Phe, Pro241Leu, Asp276Asn). Zebrafish Six2.1 shares 79% and 78% identity and 82% and 83% similarity to human and mouse Six2, respectively. GenBank accession numbers are as follows: Homo sapiens AAF69031, Mus musculus AAH68021, Danio rerio BAB40699. (B) Alignment of Bmp4 AA sequences demonstrating the identified mutations (Ser91Cys, Thr116Ser, Asn150Lys). Zebrafish Bmp4 shares 69%, 69%, and 68% identity and 80%, 80%, and 81% similarity to human, mouse, and frog Bmp4, respectively. GenBank accession numbers are as follows: Homo sapiens AAH20546, Mus musculus AAH34053, Xenopus tropicalis AAY90071, Danio rerio AAH78423.

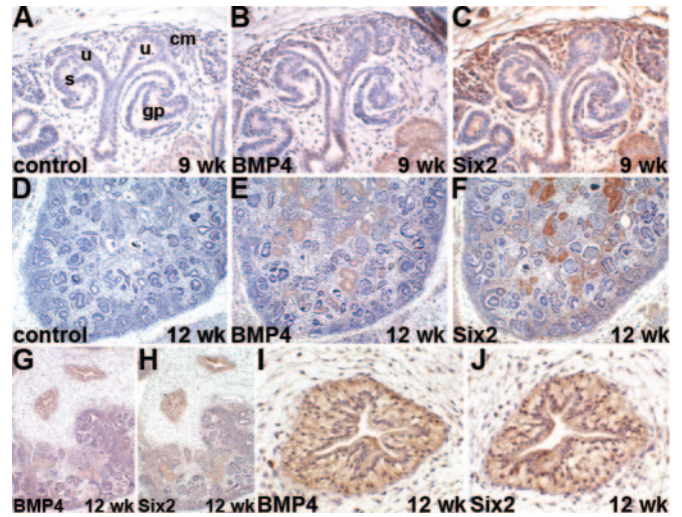


**Figure 3.** Six2 and Bmp4 expression in human fetal kidney. Immunohistochemistry for Bmp4 and Six2 in first-trimester human kidneys. All sections counterstained with hematoxylin, positive immunohistochemical signal is brown. (A-C) High power views of nephrogenic zone from 9 wk gestation kidney. (A) Branched ureteric bud tips (u), adjacent to condensing mesenchyme (cm), with deeper S-shaped body (s) and glomerular precursor (gp). (B) Only occasional cells positive for Bmp4 in mesenchyme (note light brown color within tubules in bottom right is a false positive caused by incomplete quenching of endogenous peroxidase). (C) Strongly positive signal for Six2 in uninduced mesenchyme and parts of condensed mesenchyme, ureteric buds are negative. (D) Sections through cortex of 12-wk gestation kidney (again note endogenous peroxidase). (E) Bmp4 expression is not consistently detected in the cortex at this stage. (F) Six2 is expressed in a rim of outer mesenchyme in the nephrogenic cortex. (G-J) Sections from a 12-wk gestation kidney including the medulla. (I) Higher power view of the deep medulla from panel G. (J) Higher power view of the deep medulla from panel H. Strongly positive expression of both Bmp4 and Six2 in large proximal ureteric branches in the medulla, with negative surrounding loose connective tissue. Bar = 20 μm in panels A through C, I, and J; 100 μm in D through H.

family members revealed a *de novo* mutation in patient 8 (paternity was proven by microsatellite testing as described<sup>8,16</sup>), highly suggestive of being causative. As expected, the consanguineous parents of P10 were heterozygous for the Asn150Lys mutation; their renal ultrasound was normal. A normal renal ultrasound was also demonstrated in the transmitting father of P7. The observed high variability and low penetrance of human mutations in *SIX2* and *BMP4* is in accordance with the presumed polygenic inheritance of RHD.

**SIX2 and BMP4 Are Expressed in Human Embryonic Kidney**

Immunohistochemistry was performed to determine the expression patterns of Bmp4 and Six2 in human fetal kidneys. Both Bmp4 and Six2 showed significant expression in the developing human kidneys (Figure 3). At the earliest

**Table 2.** Effect of RHD mutations on protein activity in zebrafish

RNA Injected <sup>a</sup>	RNA Concentration (pg)	Phenotype <sup>b,c</sup>			n	
		Wild-type (%)	Class I-III (%)	Class IV-V (%)		
Uninjected	NA	100	—	—	176	
<i>zsix2.1</i>	50	44	45	11	162	
	100	6	57	37	125	
<i>zsix2.1</i> L43F	50	84	12	4	138	
	100	70	23	8	105	
<i>Zsix2.1</i> Q241L	50	89	8	3	110	
	100	91	7	2	111	
<i>Zsix2.1</i> D273N	50	96	4	—	124	
	100	98	2	1	124	
		Wild-type (Class I)	Class II	Class III	Class IV	
Uninjected	NA	100	—	—	—	132
<i>zbmp4</i>	25	30	48	17	5	100
	50	32	16	36	16	44
	100	—	8	74	18	50
<i>zbmp4</i> S84C	25	69	29	—	2	126
	50	24	30	19	27	37
	100	—	—	67	33	9
<i>zbmp4</i> T109S	25	69	21	8	2	109
	50	38	13	25	25	16
	100	—	—	29	71	7
<i>zbmp4</i> D144K	25	96	4	—	—	112
	50	54	19	12	15	26
	100	26	44	30	—	27

<sup>a</sup>Differences between *six2.1* and mutated *six2.1* injection results are statistically significant at both 50 pg and 100 pg using the  $\chi^2$  test of independence. Differences between *bmp4* and mutated *bmp4* injection results are statistically significant at 25 pg only using the  $\chi^2$  test of independence (see Supplemental Table 1).

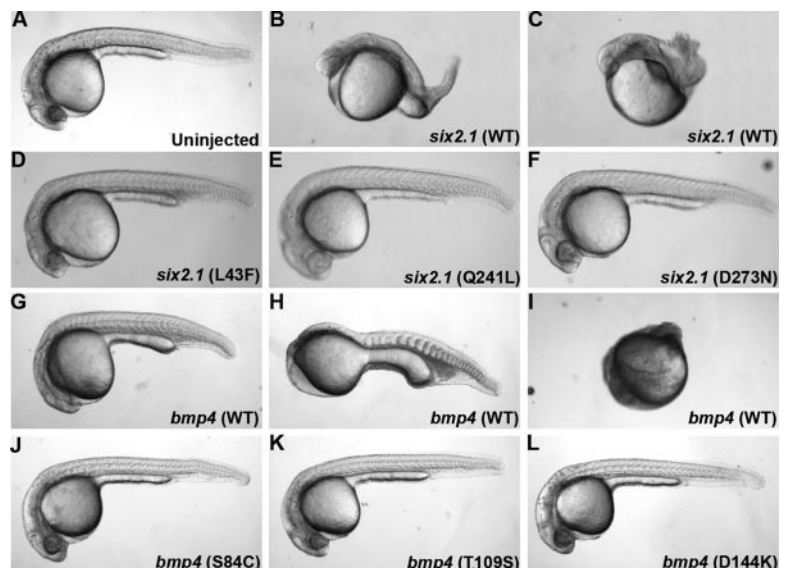
<sup>b</sup>Dorsalized phenotypes resulting from *six2.1* RNA injection were scored according to reference 52 as follows: class I-III, embryos at 24 hpf that lacked tail structures (class I and II) or had shortened twisted tails missing ventral structures (class III); class IV-V, embryos with a reduction of ventral cell types and expansion of notochord and anterior somites at 24 hpf (class IV) and bursting of embryos prior to 24 hpf due to somite expansion and constriction (class V).

<sup>c</sup>Ventralized phenotypes resulting from *bmp4* RNA injection were scored according to reference 53 as follows: class I, wild-type; class II, reduced head, expanded hematopoietic mesoderm; class III, loss of head and notochord; class IV, spindle-shaped embryo with no obvious dorsal/ventral polarity. NA, not applicable.

stage available (9 wk), Bmp4 was detected in occasional cells in the uninduced mesenchyme close to the branching tips of the ureteric bud (Figure 3, B), whereas a strong Six2 signal

was detected in virtually all cells of the uninduced mesenchyme (Figure 3, C). Six2 was also observed in a subset of cells within the condensed mesenchyme and its derivatives.

**Figure 4.** *bmp4* and *six2* overexpression phenotypes at 24 h. Lateral views of wild-type and RNA-injected zebrafish embryos at 24 h postfertilization. (A) Wild-type embryo (WT). (B-C) Embryos injected with 100 pg *six2.1* RNA demonstrating class I to III (B) and class IV (C) dorsalized phenotypes. (D-F) Embryos injected with 100 pg of mutated *six2.1* RNA: (D) *six2* L43F, (E) *six2* Q241L, (F) *six2* D273N. (G-I) Embryos injected with 25 pg *bmp4* RNA demonstrating class II (G), class III (H), and class IV (I) ventralized phenotypes. (J-L) Embryos injected with 25 pg of mutated *bmp4* RNA (J), *bmp4* S84C (K), *bmp4* T109S (L), and *bmp4* (D144K). See Table 2 for further description of ventralized and dorsalized classes.



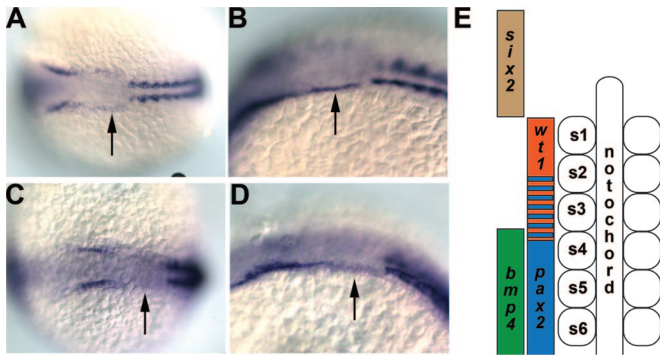


**Figure 5.** Expression of *bmp4* and *six2.1*. (A) Dorsal view of *six2.1* RNA expression in a 10-somite stage embryo. Note the expression that extends posterior from the darker stained otic placode to the first somite (arrow). (B) Lateral view of the same embryo in (A). (C) Dorsal view of *six2.1* RNA expression in a 14-somite stage embryo. Expression between the darker stained otic placode and the first somite is weaker than at 10 somites (arrow). (D) Lateral view of the same embryo in panel C. Anterior is to the left in panels A through D. Arrows denote the expression of *six2.1* that extends to the first somite. Costaining for  $\alpha$ -tropomyosin is used to indicate somites. (E) Diagram adapted from Serluca *et al.*<sup>21</sup> depicting expression domains of genes used in this study. Anterior somites are numbered from anterior (s1) to posterior (s6). *In vivo*, *bmp4*, and *six2* expression overlaps with *wt1* and *pax2.1* in the intermediate mesoderm; however, these domains are depicted laterally in this diagram for clarity.

Neither factor was observed in the epithelia of the ureteric bud, and control sections were completely negative. Similar findings were observed in the renal cortex at 12 wk of gestation (Figure 3, D through F), and sections including the medulla also demonstrated prominent immunoreactivity for both proteins in large proximal ureteric branches (Fig-

ure 3, G through J). The surrounding loose connective tissues were negative in these sections. Prominent *Bmp4* expression was observed occasionally in samples from later gestation, whereas *Six2* was still considerably expressed in the mesenchyme of the outer nephrogenic cortex (data not shown). Thus, *Bmp4* and *Six2* are expressed in the developing human kidney and have the potential to affect renal development in children.

**Human *SIX2* and *BMP4* Mutations Disrupt Protein Function**

To test for a correlation between human mutations identified in RHD and defects in protein function, we used an RNA injection assay in zebrafish. Injection of *six2.1* RNA into 1-cell zebrafish embryos resulted in dorsalization in a dose-dependent manner, suggesting a role for *six2* in dorsal mesendoderm patterning (Table 2; Figure 4). This finding is consistent with recently published data implicating *D-six4* in embryonic mesodermal patterning in *Drosophila*.<sup>17</sup> Overexpression of *bmp4* resulted in ventralization, which confirms a role of *bmp4* in ventral mesendoderm formation (Table 2; Figure 4).<sup>13,14</sup>

To assay the function of mutated *Six2.1* and *Bmp4*, the human mutations were introduced into cDNA constructs of *bmp4* and *six2.1* by site-directed mutagenesis. RNA transcribed from these constructs was injected into wild-type embryos. At doses where almost 95% of embryos showed dorsalization due to wild-type *six2.1* injection, all 3 mutant forms of *six2.1* displayed reduced activity (Table 2; Figure 4). Q241L and D273N (corresponding to human Pro241Leu and Asp276Asn) had the strongest effect on dorsalization. The effect of L43F was less dramatic, suggesting that L43F retains some residual function. Likewise, the *BMP4* mutations affected the ventralizing activity

**Table 3.** Effect of *Six2.1* and *Bmp4* morpholino injections on dorsal/ventral polarity

Morpholino Injected	Concentration (ng)	Phenotype <sup>a,b</sup>				n
		Wild-type (class I) (%)	Class II (%)	Class III (%)	Class IV (%)	
Uninjected	NA	100	0	0	0	172
<i>Six2.1</i> (ATG) <sup>c</sup>	1	89	11	0	0	113
	3	12	75	4	9	92
	6	0	30	65	4	46
	1	100	0	0	0	23
Southpaw (ATG) <sup>d</sup>	1	100	0	0	0	23
		Wild-type	Class I-III	Class IV/V		
Uninjected	NA	100	0	0	—	157
<i>Bmp4</i> (ATG) <sup>c</sup>	1	99	0	1	—	69
	3	20	56	25	—	126
	6	0	77	23	—	26
	1	100	0	0	—	23

<sup>a</sup>Dorsalized phenotypes resulting from *Bmp4* MO injection were scored according to reference 52 as follows: class I-III, embryos at 24 hpf that lacked tail structures (class I and II) or had shortened twisted tails missing ventral structures (class III); class IV-V, embryos with a reduction of ventral cell types and expansion of notochord and anterior somites at 24 hpf (class IV) and bursting of embryos prior to 24 hpf due to somite expansion and constriction (class V).

<sup>b</sup>Ventralized phenotypes resulting from *Six2.1* MO injection were scored according to reference 53 as follows: class I, wild-type; class II, reduced head, expanded hematopoietic mesoderm; class III, loss of head and notochord; class IV, spindle-shaped embryo with no obvious dorsal/ventral polarity.

<sup>c</sup>Two different morpholinos for *six2.1* and *bmp4* were injected. Because phenotypes were equivalent for both morpholinos, the data are combined.

<sup>d</sup>The southpaw morpholino gives completely penetrant phenotypes in the lateral plate mesoderm at 250 pg. Concentrations ranging from 250 pg to 2 ng have never produced dorsalized or ventralized phenotypes (this table and RDB data not shown).

NA, not applicable.

of our constructs in a dose-dependent manner. At high doses, all 4 constructs produced a high level of ventralization in most embryos. However, at lower concentrations where wild-type *bmp4* still produced significant ventralization, this ability was limited in our mutated constructs (Table 2; Figure 4). D144K (corresponding to human Asp150Lys) had the strongest effect on ventralization, whereas S84C and T109S (human Ser91Cys and Thr116Ser, respectively) had more moderate effects. Taken together, these results suggest that human mutations identified in *BMP4* and *SIX2* in human RHD patients impact normal protein function.

### Expression of Zebrafish *six2* and *bmp4*

Sequence analysis of cloned full-length zebrafish Six2.1 determined that Six2.1 shares 79% and 78% identity and 82% and 83% similarity to human and mouse Six2, respectively (Figure 2A). In zebrafish, zygotic transcription of *six2.1* begins at the 6-somite stage in the presumptive otic placode. During somitogenesis, the ectodermal expression domain extends posteriorly to the anterior border of the first somite (Figure 5). This expression is strongest from 6 to 10 somites, and fades in intensity from 12 somites on. *six2.1* expression in this area is adjacent to the area where *wilms tumor 1* (*wt1*) expression is observed in the intermediate mesoderm. At 24, 36, and 48 h after fertilization, strong *six2.1* expression is seen in the developing eye and ear consistent with expression patterns in *Drosophila* and mouse (data not shown).

The expression pattern of *bmp4* in zebrafish was reported previously.<sup>18–20</sup> Zebrafish Bmp4 shares 69%, 69%, and 68% identity and 80%, 80%, and 81% similarity to human, mouse, and frog Bmp4, respectively (Figure 2B). During somitogenesis, *bmp4* expression can be detected in the developing pronephros from the 5th somite down overlapping with areas in the intermediate mesoderm that express *pax2.1* (data not shown).<sup>20</sup>

### MO Knockdown of Six2 and Bmp4 Affects Pronephric Development

*six2.1* and *bmp4* are expressed in areas that could potentially affect the developing pronephric mesoderm in zebrafish. To determine if loss of Bmp4 and Six2 affect pronephric development, we used MO antisense oligos to knock down these proteins in zebrafish embryos. Injection of high concentrations of Bmp4 MO led to dorsalization of the embryos, consistent with the expression of *bmp4* in the ventral mesendodermal region in young embryos and the ventralization caused by overexpression of *bmp4* RNA. By contrast, injection of high concentrations of Six2.1 MO resulted in ventralization of embryos. This is in accordance with the dorsalization effect we observe when *six2.1* is overexpressed and further implicates *six2.1* in dorsal mesendoderm patterning (Table 3). However, embryos injected with low doses of the Six2.1 and Bmp4 MOs developed normally and appeared unaffected morphologically at later stages (Table 3; Figure 6).

### Expression Analysis of *wt1* and *pax2*

To determine whether pronephric development was disrupted by low doses of Bmp4 or Six2.1 MO, we analyzed the expression of the

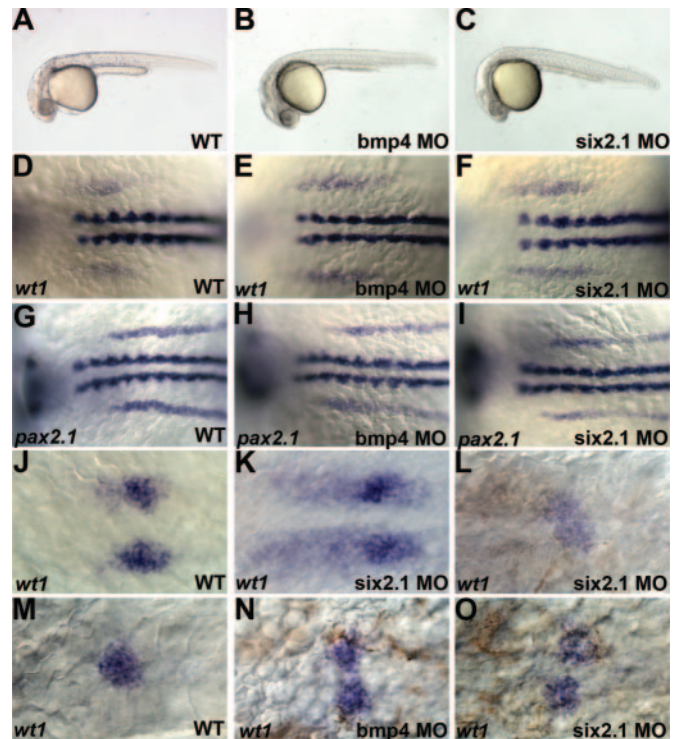


**Figure 6.** Effect of *bmp4* and *six2.1* morpholinos on pronephric development. Lateral views of wild-type (A) and embryos injected with 1 ng of *bmp4* (B) or *six2.1* (C) morpholino antisense oligonucleotides. (D–F) 6-somite stage embryos expressing *wt1*. *wt1* expression extends from the first somite to the anterior edge of the fourth somite in wild-type embryos<sup>21</sup> (D). In *bmp4* (E) or *six2.1* (F) morpholino-injected embryos, *wt1* expression extends anteriorly and posteriorly compared with wild-type. (G–I) 8-somite stage embryos expressing *pax2.1*. *pax2.1* is expressed from the third somite extending posteriorly in wild-type<sup>21</sup> (G), and this expression is unaffected in *bmp4* (H) and *six2.1* (I) morpholino-injected embryos. (J–K) *wt1* expression in glomerular precursors at 24 h postfertilization. (J) *wt1* expression condenses into two bilateral domains in wild-type (J). Additional stripes of *wt1* expression are observed in *six2.1* (K) and *bmp4* (not shown) morpholino-injected embryos. (M) *wt1* expression at 48 h postfertilization marks the fused midline glomerulus. In morpholino-injected embryos, *wt1* is observed in diffuse midline patches (L) or in unfused glomerular precursors (N–O). Anterior is to the left in all panels.

transcription factors *wt1* and *pax2.1* during early somitogenesis. Cells expressing *wt1* alone contribute to the glomerulus, cells expressing *wt1* and *pax2.1* to the pronephric tubules, and cells expressing only *pax2.1* to the pronephric tubules and duct.<sup>21</sup> While the knockdown of Six2.1 and Bmp4 had opposing effects on mesendoderm formation, knockdown of either gene had a similar effect on pronephric development (Figure 6; Table 4). At 6 to 8 somites, MO injections resulted in anterior and posterior expansion of the *wt1* expression domain, as compared with uninjected embryos. By 10 somites, anterior expansion of *wt1* expression past the first somite continued in all embryos, whereas the posterior limit of *wt1* expression was variable. The expression of *wt1* was expanded posteriorly in 30% to 50% of embryos and was truncated anteriorly in 20%. The effect on *wt1* expression

**Table 4.** Effect of Six2.1 and Bmp4 morpholino injections on zebrafish pronephric development

Morpholino Injected <sup>a</sup>	Concentration	Stage Analyzed <sup>b</sup>	Phenotypes					n
			Anterior Expansion <sup>c</sup> (%)	3s (%)	4s (%)	5s (%)	6s (%)	
<i>wt1</i> expression <sup>d</sup>								
Uninjected	NA	6–8 s	—	—	100	—	—	40
		10 s	—	—	100	—	—	21
Six2.1(ATG)	1 ng	6–8 s	100	—	27	62	11	55
		10 s	100	34	36	30	—	56
Bmp4 (ATG)	1 ng	6–8 s	100	9	23	55	13	56
		10 s	100	20	30	50	—	30
Southpaw (ATG) <sup>f</sup>	500 pg	6–8 s	—	—	100	—	—	17
		10 s	—	—	100	—	—	17
<i>pax2.1</i> expression <sup>e</sup>								
Uninjected	NA	6–8 s	—	100	—	—	—	41
		10 s	—	100	—	—	—	20
Six2.1(ATG)	1 ng	6–8 s	—	100	—	—	—	62
		10 s	—	100	—	—	—	31
Bmp4 (ATG)	1 ng	6–8 s	—	100	—	—	—	52
		10 s	—	100	—	—	—	29
<b>Glomerular <i>wt1</i> expression</b>								
			<b>Bilateral</b>	<b>Bilateral and Stripes</b>	<b>Fused</b>	<b>Unfused</b>	<b>Midline Diffuse</b>	
Uninjected	NA	24 hpf	100	—	—	—	—	37
		48 hpf	—	—	100	—	—	17
Six2.1(ATG)	1 ng	24 hpf	—	100	—	—	—	35
		48 hpf	—	—	—	82	18	17
Bmp4 (ATG)	1 ng	24 hpf	27	73	—	—	—	15
		48 hpf	—	—	—	50	50	14
Southpaw (ATG)	500 pg	24 hpf	100	—	—	—	—	26
		48 hpf	—	—	100	—	—	23

<sup>a</sup>Two different morpholinos for six2.1 and bmp4 were injected. Because phenotypes were equivalent for both morpholinos, the data are combined.

<sup>b</sup>Stages are according to references 51 and 54: s, somite; hpf, hours post fertilization.

<sup>c</sup>Expansion anterior of the first somite.

<sup>d</sup>The posterior limit of *wt1* expression is noted. *wt1* is normally expressed from 1s to 4s.

<sup>e</sup>The anterior limit of *pax2.1* is noted. *pax 2.1* is normally expressed starting at 4s and extends posteriorly throughout the intermediate mesoderm.

<sup>f</sup>The southpaw morpholino gives completely penetrant phenotypes in the lateral plate mesoderm at 250 pg. Concentrations ranging from 250 pg to 2 ng do not result in visible kidney defects.

NA, not applicable.

was specific as MO injection had no effect on *pax2.1* expression (Table 4; Figure 6). A control MO (*southpaw*) also had no effect on *wt1* expression.

Because knockdown of Six2.1 and Bmp4 specifically affected *wt1* expression, we examined the effect on glomerular development at 24 and 48 h postfertilization (hpf) (Figure 6; Table 4). At 24 hpf, *wt1* was expressed in bilateral circles representing the unfused glomerular precursors in wild-type embryos. By 48 hpf, these precursors fuse at the midline into a single glomerulus. In both Bmp4 and Six2.1 MO-injected embryos, *wt1* expression was found in stripes as well as circles at 24 hpf. At 48 hpf, the glomerular precursors either failed to fuse or formed a large diffuse and unorganized aggregate (Figure 6; Table 4). The effect on glomerular tissue is not the result of global delay of the embryos as other tissues, including the heart and visceral organs, were not affected (data not shown). In addition, these defects were not observed with a control MO (*southpaw*).

To examine the consequence of expanded *wt1* expression more closely, we sectioned morphant embryos (Figure 7). Wild-type embryos had a compact glomerulus ventral to the notochord with well-organized cell rows. Morphant embryos, however, showed disorganized *wt1* expressing cells, which were found far anterior to the normal location (Figure 7, D and E). The morphants also displayed *wt1* expressing cells that failed to fuse in the midline and to form normally organized rows (Figure 7, H and I). Thus, the knockdown of Bmp4 and Six2.1 affects both the extent of *wt1* expression in the intermediate mesoderm and thus affects the morphologic development of the glomerulus at later stages.

## DISCUSSION

### Mutational Analysis

In the present study, we provide evidence that anomalies in *SIX2* and *BMP4* are associated with defects of early kidney

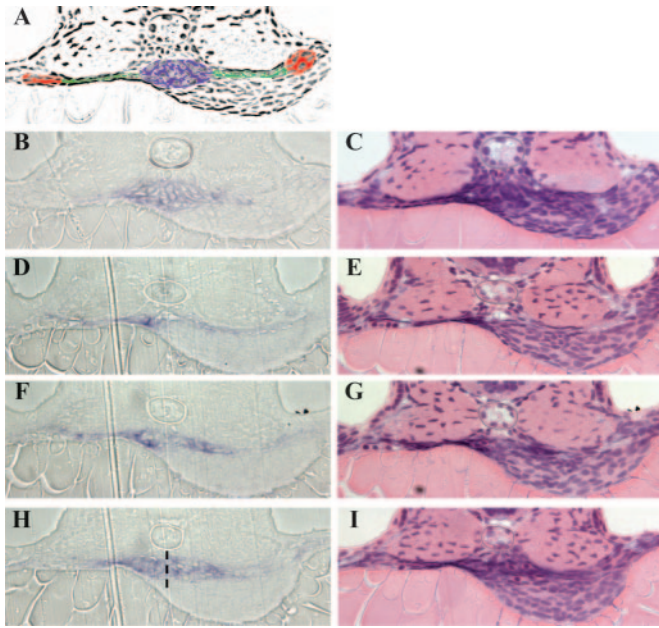


**Figure 7.** Histologic analysis of *bmp4* and *six2.1* morpholinos on pronephric development. Sections from *wt1* expressing embryos at 48 hpf. (A) Adobe Photoshop photocopy of section shown in (B and C) colored to delineate pronephric structures: glomerulus (blue), lateral tubules (green), and cross section of tubules (red). B, D, F, and H sections show *wt1* expression in blue. The same sections were processed with hematoxylin and eosin in C, E, G, and I. (B and C) wild-type embryo; *wt1* expression is compact underneath the notochord. Expression of *wt1* extends laterally into the tubules to a point approximately halfway across the somites. Note the organized rows of cells in panel B. (D–I) Three sections from a *bmp4* morphant embryo with unfused and diffuse *wt1* expression. (D and E) This section is approximately 16  $\mu$ M anterior to the normal position of the glomerulus in wild-type embryos because of the expansion of *wt1* expression. Note the expanded lateral expression of *wt1* to a point at the outer edge of the somites. (F and G) More posterior section with disorganized *wt1* expression in the glomerular and tubular regions. Expression again is expanded laterally to the edge of the somites. (H and I) Section at the expected position for the glomerulus. The two glomerular domains have failed to fuse properly; a dotted line indicated the edges of the two rounded precursor areas. Note that organized rows of cells are absent in this embryo in all 3 sections. The *wt1* expression in this embryo also extended further posteriorly than observed in wild-type embryos (data not shown).

organogenesis, reporting on the first human mutations identified in these genes so far.

The Six/Dach/Eya network plays a key role in different steps of human renal development. Members of the Six family interact with members of the Eya family in a tissue-specific fashion. The integrity of the Six-Eya complex is essential for normal renal development as evidenced by the BOR syndrome, which is the result of haploinsufficiency of *EYA1*, *SIX1* or *SIX5*, respectively.<sup>7,8,22</sup> Because of the strong overlap of *Six1* and *Six2* expression patterns during early steps of nephrogenesis, *Six2* also seemed likely to be involved in the development of the

kidney, and it was demonstrated that the murine knockout of *Six2* is associated with severe dysplasia of the kidneys.<sup>4</sup> Two *Six2* binding sites were identified within the promoter of the *Gdnf* gene, and it was demonstrated that *Six2* strongly activates the expression of *Gdnf* *in vitro*.<sup>11</sup> In the present study, mutations in *SIX2* were identified in 5 unrelated subjects, one mutation affecting a conserved amino acid residue of the Eya-binding SD and 2 mutations locating to the *SIX2*-specific CD. Interestingly, the Pro241Leu exchange identified in 3 different unrelated patients is predicted to destroy a SH3 binding site in *Six2* that might be involved in protein-protein-complex formation. In contrast to the patients affected by *SIX1* mutations who also present with otic defects, the patients affected by *SIX2* mutations did not exhibit any extrarenal symptoms. This is possibly explained by functional redundancy due to the otic expression of other members of the Six family, e.g., *Six4*.<sup>23</sup>

First genetic analyses of human *BMP4* were performed by Nakano *et al.*<sup>24</sup> in 7 congenital anomalies of the kidney and urinary tract patients, but no mutations were identified. In the present study of 250 patients, 3 human *BMP4* mutations (Ser91Cys, Thr116Ser, and Asn150Lys) are described for the first time in 5 patients with congenital anomalies of the kidney. All mutations affect highly conserved residues of the *Bmp4* prodomain. *Bmp4* is synthesized as a preproprotein from which a prodomain is cleaved, which serves to stabilize the mature *Bmp4* protein.<sup>25</sup> *In vitro* studies demonstrated that mutations that affect prodomain cleavage target *Bmp4* for degradation.<sup>26</sup> While the mutations identified in the present study do not directly affect the cleavage sites, they likely affect the conformation of the prodomain, potentially interfering with prodomain cleavage and/or stabilization of the mature protein. Mutations in other members of the TGF- $\beta$  family also affecting the prodomain support the relevance of this domain for intact mature protein function. For example, a dominant missense mutation affecting the prodomain of *Bmp15* causes autosomal dominant ovarian dysgenesis,<sup>27</sup> and *TGFB1* mutations that are localized in the prodomain of TGF- $\beta$ 1 lead to autosomal dominant diaphyseal dysplasia (Camurati-Engelmann disease).<sup>28</sup>

The patients affected by gene mutations in either *SIX2* or *BMP4* showed a broad spectrum of severe kidney malformations, including hypoplastic, dysplastic, or cystic dysplastic kidneys (unilateral or bilateral, with/or without VUR). This observed variation in the phenotypic presentation is in accordance with the budding theory,<sup>3,29</sup> assuming that disturbed UB during nephrogenesis is associated with the development of kidneys that are too small and/or dysplastic and may have refluxive or obstructive ureters. As both *Six2* and *Bmp4* participate in the reciprocal interactions of UB, their dysfunction seems a convincing explanation for establishing a predisposition in affected mutation carriers to develop RHD.

These results are further supported by the confirmed expression of *Bmp4* and *Six2* in human renal tissue. In human fetal kidneys, *Bmp4* expression was notably observed in the large proximal ureteric branches of the medulla and in a subset of cells in the

uninduced mesenchyme of the nephrogenic cortex close to the branching tips of the ureteric bud, as could have been expected. The expression of Bmp4 appeared different to the pattern observed in mice,<sup>12,30</sup> as no expression was observed in Bowman's capsules or proximal tubules at these early stages where its expression was reported by Dudley *et al.*<sup>30</sup> Therefore expression may change during human gestation or as Bmp4 is a secreted molecule, some of these differences might be explained by the fact that Dudley and Robertson examined the mRNA expression of Bmp4 rather than the expression of the protein. For Six2, the protein distribution was very similar in humans to the reported mRNA location in murine kidneys.<sup>4,31</sup> Its major site of expression was in the uninduced mesenchyme in the nephrogenic cortex, with a reduced expression in the induced mesenchyme and its derivatives. We also noted Six2 in large proximal ureteric branches in the medulla, where its expression overlapped with Bmp4. The expression pattern of both proteins is therefore consistent with important functions in early nephrogenesis, not only in mice which has formerly been suggested by respective knockout mouse models but also in humans supporting a role for Bmp4 and Six2 in congenital anomalies of the kidney and urinary tract pathogenesis in children.

### Overexpression Assay

The zebrafish has become an increasingly important model system to understand the molecular genetic basis of vertebrate organogenesis, including the development of the kidneys. Nephrogenesis in the zebrafish has a remarkable degree of similarity of organ cell types compared with higher vertebrates and numerous gene mutants have a correlate in human renal disease.<sup>32–35</sup> We demonstrate that the mutations identified in RHD patients reduce or eliminate the function of Six2 and Bmp4 in a zebrafish overexpression assay. A similar approach has been used to confirm that human mutations in *CFC1* and *TDGF1* result in loss of protein function.<sup>36,37</sup> Human mutations introduced into *six2.1* and *bmp4* strongly affect the ability of injected RNA to dorsalize or ventralize zebrafish embryos, respectively. At physiologic levels in an embryo, these mutations might have profound effects at multiple steps in kidney development, cumulatively leading to the defects observed in RHD patients.

### MO Knockdown

While naturally occurring *bmp4* and *six2.1* mutations in zebrafish have yet to be described, targeting of antisense MOs<sup>38</sup> to prevent RNA translation of these gene products is an effective approach to knockdown gene function.

We provide evidence that knockdown of Bmp4 and Six2.1 in zebrafish affects the pronephric expression of *wt1* and subsequently glomerular morphogenesis. *bmp4* is expressed in the developing pronephric mesoderm in zebrafish,<sup>20</sup> and overexpression of *bmp4* has been shown to expand the expression of *pax2.1* in this tissue.<sup>39</sup> Our results show that knockdown of *bmp4* leads to an expansion of *wt1* expression into the domain that normally expresses *pax2.1* consistent with a role for *bmp4* in maintaining the boundary between the *wt1* and *pax2.1* ex-

pression domains. *six2.1* is expressed in tissue adjacent to the anterior boundary of *wt1* expression and our results suggest that it acts in a nonautonomous fashion to limit the *wt1* expressing pronephric mesoderm. It is interesting to note that in zebrafish we see expression of these genes surrounding the area that will become the glomerulus, but not within the glomerulus itself. In human tissue, we also noted higher expression in uninduced mesenchyme. Thus, we speculate that these genes may act to define a progenitor area or keep mesenchyme in an undifferentiated state.

### Bmp4 and Six2 in Zebrafish and Human Kidney Development

Renal hypodysplasia of the human kidney is characterized by maldevelopment and disturbed mesenchyme differentiation; therefore, both zebrafish and human kidneys in a Bmp4 or Six2 mutant state show defects in general structural formation and in the final differentiation steps. The zebrafish phenotype observed in MO-injected embryos includes malformations where the nephron does not form correctly and the morphology of the kidney is considerably altered. Our results suggest that Bmp4 and Six2 can affect renal development from the earliest pronephric formation (zebrafish data) to the final metanephric kidney in mammals (human data).

Intriguingly, the effect on the pronephros is identical for the knockdown of either *bmp4* or *six2.1*, while the evidence suggests these genes act in opposing fashions on early mesoderm patterning. It remains unclear how *six2.1* and *bmp4* act in patterning the pronephros, but recent papers hint at links between *six* genes and *bmp* regulation: *bmp4* expression is downregulated in otic vesicles in *dog-eared* (*eya1*) mutant zebrafish embryos,<sup>40</sup> and *six3* has been shown to repress *bmp4* transcription directly in *Xenopus* and zebrafish during anterior neural plate specification.<sup>41</sup> It is worth noting that while *bmp4* and *six2.1* are expressed at the right place and time to affect pronephric development during somite stages, knockdown of *bmp4* and *six2.1* could also be affecting pronephric development by altering global mesoderm patterning in the early embryo leading to an expansion of the intermediate mesoderm region that will express *wt1*. However, the MO-injected embryos we analyzed did not show global mesoderm patterning defects nor alterations of *pax2.1* in the intermediate mesoderm (Figure 6; data not shown), suggesting the observed effects were due to later functions of *bmp4* and *six2.1* in pronephric development.

The fact that both genes are expressed at multiple developmental stages indicates that mutations in these genes might also affect human kidney development at multiple steps from mesoderm patterning through metanephric induction. Thus, cumulative effects of mutations at each step are likely to contribute to the variable phenotype observed in the affected patients. This is in agreement with the assumption that the pathogenesis of RHD might be related to multifactorial and/or polygenic actions involving Six2 and Bmp4 as 2 players in a complex system and constitutes a stringent explanation of the observed incomplete penetrance in parental heterozygous mutation carriers. A lethal effect was ob-

served by introducing homozygous *Six2* and *Bmp4* gene knock-outs in mice<sup>4,12,42</sup>; because isoforms of both genes have important functions also for the development of nonrenal tissues, we speculate that human *SIX2* and *BMP4* loss-of-function mutations may be associated with a phenotype much more severe than RHD. However, it seems likely that nonlethal mutations in key developmental genes are involved in an imbalancing of factors that regulate the budding of the ureter and the differentiation of the kidney, thereby predisposing to developmental fragility. Following this idea, the additive effect of sequence variants in individual developmental genes results in a latent predisposition to develop RHD, which realizes if several factors are superposed.

## CONCISE METHODS

### Patients

A total of 250 children with RHD phenotype and impaired renal function were selected for mutational analysis in *SIX2* and *BMP4*. RHD was defined by the presence of small (<3rd percentile) and/or disorganized kidneys with/without cysts on ultrasound. Patients with ureteral anomalies and/or isolated VUR but kidneys of normal sonographic size and structure, as well as patients with bladder or urethral abnormalities were excluded.

The study was approved by the ethical committees in all participating centers and informed assent and/or consent for genetic screening was obtained from the patients and/or parents as appropriate. A total of 150 race-matched individuals, unrelated to the patients, served as controls.

### Mutation Screening

Genomic DNA was extracted from peripheral blood leukocytes by standard methods. Overlapping sets of primers based on the sequence of the human *SIX2* and *BMP4* genes were used to amplify the coding sequences of the genomic DNA by PCR. Mutation screening was performed by denaturing HPLC (WAVE System) or single-strand conformation polymorphism analysis (Multiphor II, Amersham Biosciences, Piscataway, NJ). When abnormal migration patterns were detected, direct sequencing on both strands was performed by applying the fluorometric method (ABI 3700 DNA sequencer, Applied Biosystems, Foster City, CA). *PAX2* and *EYA1* mutations were excluded in all patients affected by *SIX2* or *BMP4* mutations by direct sequencing. Primer sequences are available upon request.

### Human Tissues

Phenotypically normal human kidney samples were obtained from two sources: (1) chemically induced terminations of pregnancy between 9 to 12 wk of gestation ( $n = 6$ ), collected by the Wellcome Trust and Medical Research Council-funded Human Developmental Biology Resource at the UCL Institute of Child Health and (2) later miscarriages or terminations of pregnancy between 18 and 24 wk of gestation obtained from the Pathology Department of the University College London Medical School ( $n = 4$ ). Informed consent to analyze these samples was obtained from the mothers involved, and use was

approved by the Joint University College London/University College Hospital Committee on the Ethics of Human Research.

### Immunohistochemistry on Human Kidney Tissue

Human tissues were processed using standard techniques for paraffin wax-based sections, and then subjected to conventional immunohistochemistry, as described.<sup>43</sup> The antibody against *Bmp4* was a mouse monoclonal antibody (NCL-BMP4; Novocastra, Newcastle Upon Tyne, UK) used in a 1:10 dilution, and for *Six2* was a rabbit polyclonal antibody (PA1-17185; Affinity Bioreagents, Golden, CO) used in a 1:200 dilution. Primary antibodies were omitted in the negative controls.

### RNA In Situ Hybridization Studies in Zebrafish Embryos

RNA *in situ* hybridization was performed using standard techniques<sup>44</sup> with the following antisense probes: *six2.1* (this paper), *bmp4*,<sup>20</sup> *wt1a*,<sup>21,45</sup> *pax2.1*,<sup>46</sup> and  $\alpha$ -*tropomyosin*.<sup>47</sup> Embryos were mounted in modified GMM mounting media<sup>48</sup> (100 ml Canada Balsam, Sigma-Aldrich, St. Louis, MO; + 10 ml methyl salicylate, Sigma-Aldrich, St. Louis, MO) and photographed on a Leica DMRA scope equipped with a ProgRes C14 camera. Images were adjusted for brightness and contrast in Adobe Photoshop, version 7.0. For histologic analysis, embryos were embedded in JB4 resin and sectioned. *wt1* expression was photographed followed by processing of sections with hematoxylin and eosin (detailed protocols available upon request).

### cDNA Cloning of *Danio rerio six2.1*

Full-length sequence for zebrafish *six2.1* was obtained by BLAST search of the TIGR database. The sequence from TIGR cluster TC293555 was used to design primers for nested PCR from a 24-h cDNA library. Primer sequences: *six2.1* F1 GCCACCAGTTCTC-CCCGCACA, *six2.1*F2 CTGGTCCCAGCGCCATCCCA, *six2.1*R1 TGTGCGGGGAGAACTGGTGGC and *six2.1*R2 TGGGATG-GCGCTGGGACCAG. *six2.1* was cloned into Bluescript II SK(-) (Stratagene, La Jolla, CA) for probe production and into T7TS vector<sup>49</sup> for messenger RNA production. To minimize potential differences in expression of our constructs, at least two preparations of RNA were generated for each construct and concentrations determined by spectrophotometry. Injections were performed with RNA from each preparation to control for batch to batch variability in RNA. RNA injections were performed at least three separate times to control for any variability in injections.

### Site-Directed Mutagenesis and Construct Design

Mutations in *six2.1* and *bmp4* cDNAs were generated using QuikChange II Site Directed Mutagenesis Kit (Stratagene). Capped mRNAs from wild-type and mutated constructs were transcribed using mMessage mMachine Transcription Kit (Ambion, Austin, TX) for injection.

### Injections and MO Experiments in Zebrafish Embryos

All experiments were performed following NIH guidelines for the care and use of laboratory animals. RNA and MO injections were performed as described.<sup>50</sup> MOs were resuspended in dH<sub>2</sub>O at a concentration of 50  $\mu\text{g}/\mu\text{l}$  and diluted into 5 mg/ml phenol red in 0.1 mM KCL solution for injection. We controlled for nonspecific effects of

MOs by generating two different MOs for zebrafish *six2.1* and *bmp4*. Since the phenotypes were indistinguishable for both MOs to *bmp4* or *six2.1*, the effects we see are likely the result of specific knockdown of these genes. We have combined the results for the 2 different MOs in "Results." As a control for nonspecific effects, we injected a MO to *southpaw*, which specifically affects the lateral plate mesoderm,<sup>51</sup> and analyzed pronephric development. Analysis of pronephric development was performed in embryos injected with low doses of MO. Only embryos that developed indistinguishable from wild-type controls were evaluated in this study. MO sequences are as follows: *six2.1*ATG - GTCTCGACAGAAGATAAAGCATGGG, *six2.1*#2ATG - TTGTCTCAAAAATAAACGTCCCTCT, *bmp4*ATG - AGCCGAATGTTGGAAGCATAGACAT, and *bmp4*#2ATG - AACAGTCCATGTTTGTGAGAGGTG.

### Statistical Analyses

Statistical analyses of protein structures and amino acid composition, sequence alignments, and similarity searches were conducted using software and databases provided by Infobiogen (www.infobiogen.fr), ENSEMBL (www.ensembl.org), TIGR database (www.tigr.org), and the National Center for Biotechnical Information (www.ncbi.nlm.nih.gov). Statistical analysis prediction of protein SH3 binding sites was performed by Scansite (http://scansite.mit.edu). The significance of injection results was determined using the  $\chi^2$  test of independence.

### ACKNOWLEDGMENTS

This study was supported by the European Commission (5th Framework Programme, QLGI-CT-2002-00908), the Deutsche Forschungsgemeinschaft (WE 2724/2 to 2), the Boehringer Ingelheim Foundation, the Baxter Extramural Grant Program, and the Kuratorium für Dialyse und Nierentransplantation. R.D.B. is the 44th Mallinckrodt Scholar and supported by the Edward Mallinckrodt Jr. Foundation grant award.

The authors thank the patients and their families for kindly participating in this study.

### Appendix

ESCAPE trial participants: A. Anarat (Adana); A. Bakkaloglu, F. Ozaltin (Ankara); A. Peco-Antic (Belgrade); U. Querfeld, J. Gellermann (Berlin); P. Sallay (Budapest); D. Drozd (Cracow); K.-E. Bonzel, A.-M. Wingen (Essen); A. Zurowska, I. Balasz (Gdansk); F. Perfumo, A. Canepa (Genoa); D.E. Müller-Wiefel, K. Zepf (Hamburg); G. Offner, B. Enke (Hannover); O. Mehls, F. Schaefer, E. Wühl, C. Hadtstein (Heidelberg); U. Berg, G. Celsi (Huddinge); S. Emre, A. Sirin, I. Bilge (Istanbul); S. Çaliskan (Istanbul-Cerrahpasa); S. Mir, E. Serdaroglu (Izmir); C. Greiner, H. Eichstädt, S. Wygoda (Leipzig); K. Hohbach-Hohenfellner (Mainz); N. Jeck, G. Klaus (Marburg); A. Appiani, G. Ardissino, S. Testa (Milano); G. Montini (Padova); C. Antignac, P. Niaudet, M. Charbit (Paris); J. Dusek (Prague); A. Caldas-Afonso, A. Teixeira (Porto); S. Picca, C. Matteucci (Rome); M. Wigger (Rostock); M. Fischbach, J. Terzic (Strasbourg); J. Fydryk, T. Urasinski (Szczecin); R. Coppo, L. Peruzzi (Torino); A. Jankauskiene

(Vilnius); M. Litwin, M. Abuauaba, R. Grenda (Warszawa); K. Arbeiter (Vienna); and T.J. Neuhaus (Zurich).

### DISCLOSURES

None.

### REFERENCES

1. Woolf AS: A molecular and genetic view of human renal and urinary tract malformations. *Kidney Int* 58: 500–512, 2000
2. Woolf AS, Price KL, Scambler PJ, Winyard PJ: Evolving concepts in human renal dysplasia. *J Am Soc Nephrol* 15: 998–1007, 2004
3. Piscione TD, Rosenblum ND: The molecular control of renal branching morphogenesis: current knowledge and emerging insights. *Differentiation* 70: 227–246, 2002
4. Self M, Lagutin OV, Bowling B, Hendrix J, Cai Y, Dressler GR, Oliver G: Six2 is required for suppression of nephrogenesis and progenitor renewal in the developing kidney. *EMBO J* 25: 5214–5228, 2006
5. Ghanbari H, Seo HC, Fjose A, Brandli AW: Molecular cloning and embryonic expression of *Xenopus Six* homeobox genes. *Mech Dev* 101: 271–277, 2001
6. Ohto H, Takizawa T, Saito T, Kobayashi M, Ikeda K, Kawakami K: Tissue and developmental distribution of Six family gene products. *Int J Dev Biol* 42: 141–148, 1998
7. Ruf RG, Xu PX, Silvius D, Otto EA, Beekmann F, Muerb UT, Kumar S, Neuhaus TJ, Kemper MJ, Raymond RM, Jr., Brophy PD, Berkman J, Gattas M, Hyland V, Ruf EM, Schwartz C, Chang EH, Smith RJ, Stratakis CA, Weil D, Petit C, Hildebrandt F: SIX1 mutations cause branchio-oto-renal syndrome by disruption of EYA1-SIX1-DNA complexes. *Proc Natl Acad Sci U S A* 101: 8090–8095, 2004
8. Hoskins BE, Cramer CH, Silvius D, Zou D, Raymond RM, Orten DJ, Kimberling WJ, Smith RJ, Weil D, Petit C, Otto EA, Xu PX, Hildebrandt F: Transcription factor SIX5 is mutated in patients with branchio-oto-renal syndrome. *Am J Hum Genet* 80: 800–804, 2007
9. Schwab K, Patterson LT, Aronow BJ, Luckas R, Liang HC, Potter SS: A catalogue of gene expression in the developing kidney. *Kidney Int* 64: 1588–1604, 2003
10. Durbec P, Marcos-Gutierrez CV, Kilkenny C, Grigoriou M, Wartiovaara K, Suvanto P, Smith D, Ponder B, Costantini F, Saarma M, Sariola H, Pachnis V: GDNF signalling through the Ret receptor tyrosine kinase. *Nature* 381: 789–793, 1996
11. Brodbeck S, Besenbeck B, Englert C: The transcription factor Six2 activates expression of the *Gdnf* gene as well as its own promoter. *Mech Dev* 121: 1211–1222, 2004
12. Miyazaki Y, Oshima K, Fogo A, Hogan BL, Ichikawa I: Bone morphogenetic protein 4 regulates the budding site and elongation of the mouse ureter. *J Clin Invest* 105: 863–873, 2000
13. von Bubnoff A, Cho KW: Intracellular BMP signaling regulation in vertebrates: pathway or network? *Dev Biol* 239: 1–14, 2001
14. Hogan BL: Bone morphogenetic proteins in development. *Curr Opin Genet Dev* 6: 432–438, 1996
15. Miyazaki Y, Oshima K, Fogo A, Ichikawa I: Evidence that bone morphogenetic protein 4 has multiple biological functions during kidney and urinary tract development. *Kidney Int* 63: 835–844, 2003
16. Schonfelder EM, Knuppel T, Tasic V, Miljkovic P, Konrad M, Wuhl E, Antignac C, Bakkaloglu A, Schaefer F, Weber S: Mutations in Uroplakin IIIA are a rare cause of renal hypodysplasia in humans. *Am J Kidney Dis* 47: 1004–1012, 2006
17. Clark IB, Boyd J, Hamilton G, Finnegan DJ, Jarman AP: D-six4 plays a key role in patterning cell identities deriving from the Drosophila mesoderm. *Dev Biol* 294: 220–231, 2006

18. Martinez-Barbera JP, Toresson H, Da Rocha S, Krauss S: Cloning and expression of three members of the zebrafish Bmp family: Bmp2a, Bmp2b and Bmp4. *Gene* 198: 53–59, 1997
19. Hwang SP, Tsou MF, Lin YC, Liu CH: The zebrafish BMP4 gene: sequence analysis and expression pattern during embryonic development. *DNA Cell Biol* 16: 1003–1011, 1997
20. Chin AJ, Chen JN, Weinberg ES: Bone morphogenetic protein-4 expression characterizes inductive boundaries in organs of developing zebrafish. *Dev Genes Evol* 207: 107–114, 1997
21. Serluca FC, Fishman MC: Pre-pattern in the pronephric kidney field of zebrafish. *Development* 128: 2233–2241, 2001
22. Abdelhak S, Kalatzis V, Heilig R, Compain S, Samson D, Vincent C, Weil D, Cruaud C, Sahly I, Leibovici M, Bitner-Glindzicz M, Francis M, Lacombe D, Vigneron J, Charachon R, Boven K, Bedbeder P, Van Regemorter N, Weissenbach J, Petit C: A human homologue of the Drosophila eyes absent gene underlies branchio-oto-renal (BOR) syndrome and identifies a novel gene family. *Nat Genet* 15: 157–164, 1997
23. Streit A: Extensive cell movements accompany formation of the otic placode. *Dev Biol* 249: 237–254, 2002
24. Nakano T, Niimura F, Hohenfellner K, Miyakita E, Ichikawa I: Screening for mutations in BMP4 and FOXC1 genes in congenital anomalies of the kidney and urinary tract in humans. *Tokai J Exp Clin Med* 28: 121–126, 2003
25. Cui Y, Hackenmiller R, Berg L, Jean F, Nakayama T, Thomas G, Christian JL: The activity and signaling range of mature BMP-4 is regulated by sequential cleavage at two sites within the prodomain of the precursor. *Genes Dev* 15: 2797–2802, 2001
26. Degnin C, Jean F, Thomas G, Christian JL: Cleavages within the prodomain direct intracellular trafficking and degradation of mature bone morphogenetic protein-4. *Mol Biol Cell* 15: 5012–5020, 2004
27. Di Pasquale E, Beck-Peccoz P, Persani L: Hypergonadotropic ovarian failure associated with an inherited mutation of human bone morphogenetic protein-15 (BMP15) gene. *Am J Hum Genet* 75: 106–111, 2004
28. Kinoshita A, Saito T, Tomita H, Makita Y, Yoshida K, Ghadami M, Yamada K, Kondo S, Ikegawa S, Nishimura G, Fukushima Y, Nakagomi T, Saito H, Sugimoto T, Kamegaya M, Hisa K, Murray JC, Taniguchi N, Niikawa N, Yoshiura K: Domain-specific mutations in TGFB1 result in Camurati-Engelmann disease. *Nat Genet* 26: 19–20, 2000
29. Ichikawa I, Kuwayama F, Pope JC, Stephens FD, Miyazaki Y: Paradigm shift from classic anatomic theories to contemporary cell biological views of CAKUT. *Kidney Int* 61: 889–898, 2002
30. Dudley AT, Robertson EJ: Overlapping expression domains of bone morphogenetic protein family members potentially account for limited tissue defects in BMP7 deficient embryos. *Dev Dyn* 208: 349–362, 1997
31. Oliver G, Wehr R, Jenkins NA, Copeland NG, Chetty BN, Hartenstein V, Zipursky SL, Gruss P: Homeobox genes and connective tissue patterning. *Development* 121: 693–705, 1995
32. Hostetter CL, Sullivan-Brown JL, Burdine RD: Zebrafish pronephros: a model for understanding cystic kidney disease. *Dev Dyn* 228: 514–522, 2003
33. Drummond IA: Kidney development and disease in the zebrafish. *J Am Soc Nephrol* 16: 299–304, 2005
34. Drummond I: The pronephros. *Results Probl Cell Differ* 40: 322–345, 2002
35. Drummond IA: The zebrafish pronephros: a genetic system for studies of kidney development. *Pediatr Nephrol* 14: 428–435, 2000
36. de la Cruz JM, Bamford RN, Burdine RD, Roessler E, Barkovich AJ, Donnai D, Schier AF, Muenke M: A loss-of-function mutation in the CFC domain of TDGF1 is associated with human forebrain defects. *Hum Genet* 110: 422–428, 2002
37. Bamford RN, Roessler E, Burdine RD, Saplakoglu U, dela Cruz J, Splitt M, Goodship JA, Towbin J, Bowers P, Ferrero GB, Marino B, Schier AF, Shen MM, Muenke M, Casey B: Loss-of-function mutations in the EGF-CFC gene CFC1 are associated with human left-right laterality defects. *Nat Genet* 26: 365–369, 2000
38. Nasevicius A, Ekker SC: Effective targeted gene “knockdown” in zebrafish. *Nat Genet* 26: 216–220, 2000
39. Neave B, Holder N, Patient R: A graded response to BMP-4 spatially coordinates patterning of the mesoderm and ectoderm in the zebrafish. *Mech Dev* 62: 183–195, 1997
40. Kozłowski DJ, Whitfield TT, Hukriede NA, Lam WK, Weinberg ES: The zebrafish dog-eared mutation disrupts *eya1*, a gene required for cell survival and differentiation in the inner ear and lateral line. *Dev Biol* 277: 27–41, 2005
41. Gestri G, Carl M, Appolloni I, Wilson SW, Barsacchi G, Andreazzoli M: Six3 functions in anterior neural plate specification by promoting cell proliferation and inhibiting Bmp4 expression. *Development* 132: 2401–2413, 2005
42. Dunn NR, Winnier GE, Hargett LK, Schrick JJ, Fogo AB, Hogan BL: Haploinsufficient phenotypes in Bmp4 heterozygous null mice and modification by mutations in Gli3 and Alx4. *Dev Biol* 188: 235–247, 1997
43. Price KL, Long DA, Jina N, Liapis H, Hubank M, Woolf AS, Winyard PJ: Microarray interrogation of human metanephric mesenchymal cells highlights potentially important molecules in vivo. *Physiol Genomics* 28: 193–202, 2007
44. Thisse C, Thisse B, Schilling TF, Postlethwait JH: Structure of the zebrafish *snail1* gene and its expression in wild-type, spadetail and no tail mutant embryos. *Development* 119: 1203–1215, 1993
45. Bollig F, Mehringer R, Perner B, Hartung C, Schafer M, Schartl M, Volff JN, Winkler C, Englert C: Identification and comparative expression analysis of a second *wt1* gene in zebrafish. *Dev Dyn* 235: 554–561, 2006
46. Krauss S, Johansen T, Korzh V, Fjose A: Expression of the zebrafish paired box gene *pax[zf-b]* during early neurogenesis. *Development* 113: 1193–1206, 1991
47. Ohara O, Dorit RL, Gilbert W: One-sided polymerase chain reaction: the amplification of cDNA. *Proc Natl Acad Sci U S A* 86: 5673–5677, 1989
48. Struhl G: Anterior and posterior compartments in the proboscis of Drosophila. *Dev Biol* 84: 372–385, 1981
49. Cleaver OB, Patterson KD, Krieg PA: Overexpression of the tinman-related genes *XNkx-2.5* and *XNkx-2.3* in *Xenopus* embryos results in myocardial hyperplasia. *Development* 122: 3549–3556, 1996
50. Gritsman K, Zhang J, Cheng S, Heckscher E, Talbot WS, Schier AF: The EGF-CFC protein one-eyed pinhead is essential for nodal signaling. *Cell* 97: 121–132, 1999
51. Long S, Ahmad N, Rebagliati M: The zebrafish nodal-related gene *southpaw* is required for visceral and diencephalic left-right asymmetry. *Development* 130: 2303–2316, 2003
52. Mullins MC, Hammerschmidt M, Kane DA, Odenthal J, Brand M, van Eeden FJ, Furutani-Seiki M, Granato M, Haffter P, Heisenberg CP, Jiang YJ, Kelsh RN, Nusslein-Volhard C: Genes establishing dorsoventral pattern formation in the zebrafish embryo: the ventral specifying genes. *Development* 123: 81–93, 1996
53. Schmid B, Furthauer M, Connors SA, Trout J, Thisse B, Thisse C, Mullins MC: Equivalent genetic roles for *bmp7/snailhouse* and *bmp2b/swirl* in dorsoventral pattern formation. *Development* 127: 957–967, 2000
54. Kimmel CB, Ballard WW, Kimmel SR, Ullmann B, Schilling TF: Stages of embryonic development of the zebrafish. *Dev Dyn* 203: 253–310, 1995

See related editorial, “Some Assembly Required: Renal Hypodysplasia and the Problem with Faulty Parts,” on pages 834–836.

Supplemental information for this article is available online at <http://www.jasn.org/>.